Письма в ЭЧАЯ. А. 2011. Т. 8, № 9. С. 75–83

SEARCH FOR THE CRITICAL POINT OF STRONGLY INTERACTING MATTER AT THE CERN SPS

P. Seyboth
for the NA49 and NA61 Collaborations
Max-Planck-Institut für Physik, Munich, Germany
Jan Kochanowski University, Kielce, Poland

The study of central collisions of heavy nuclei at CERN SPS energies by NA49 provided evidence for the onset of deconfinement around 30A GeV. Theoretical considerations predict a critical point of strongly interacting matter accessible in the SPS energy range. A search for the expected fluctuations has not yet found convincing signals. The strategy and plans for the continuation of this program at the SPS by NA61 with lighter nuclei are discussed.

PACS: 25.75.-q

INTRODUCTION

Relativistic heavy-ion collisions have been widely used to study the properties of matter at extreme temperatures and densities. Under such conditions quantum chromodynamics (QCD) predicts a phase transition between a hadron gas and a state of quasi-free quarks and gluons,

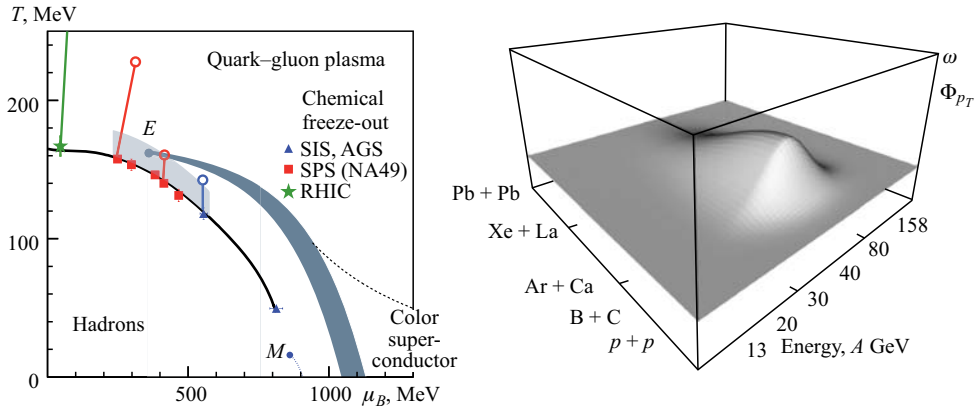

Fig. 1. *a*) Phase diagram of strongly interacting matter with locations of freeze-out of the hadron composition (as determined from statistical model fits [9, 10]) in central Pb + Pb (Au + Au) collisions at RHIC (star), SPS (squares), AGS and SIS (triangles). The shaded band indicates the first-order phase boundary and E its critical endpoint as estimated by lattice QCD [4]. *b*) Schematic plot of the intensity of average transverse momentum (Φ_{pT}) and multiplicity (ω) fluctuations near the critical point. The baryochemical potential μ_B decreases with increasing beam energy, the freeze-out temperature T increases with decreasing size of the colliding nuclei

the quark–gluon plasma (QGP). Exploration of the phase diagram of strongly interacting matter (Fig. 1, *a*) remains of fundamental interest.

Motivated by the predictions of the Statistical Model of the Early Stage (SMES) [1], an energy scan of nucleus–nucleus collisions was performed by the NA49 experiment at the CERN SPS in order to locate the onset of deconfinement. Final results from these studies [2,3] will be summarized.

QCD suggests that the phase boundary between QGP and hadrons is of first order at high baryon density, ends in a critical point (see Fig. 1, *a*), and then turns into a rapid crossover at low baryon density [4]. In the vicinity of the critical point large fluctuations are expected [5–7] as illustrated by Fig. 1, *b*. The status of the search for such fluctuations at the SPS by the NA49 experiment will be reviewed. Finally, the strategy and plans of the NA61 experiment [8] for the continuation of this program with lighter nuclei will be discussed.

1. ONSET OF DECONFINEMENT IN THE SPS ENERGY RANGE

The energy dependence of various hadron production properties was shown to indicate when the produced matter droplet initially reaches deconfinement [1]. Rapid changes were found near $30A$ GeV in the energy scan of central Pb + Pb collisions which covered SPS beam energies of $20A$, $30A$, $40A$, $80A$, and $158A$ GeV ($\sqrt{s_{NN}} = 6.3, 7.6, 8.7, 12.3$ and 17.3 GeV). The increase of the pion yield per participating nucleon clearly steepens in the SPS energy region (see Fig. 2, *a*). In a statistical model scenario this can be interpreted as an increase of the effective degrees of freedom [1] by a factor ≈ 3 [2], consistent with the activation of quark–gluon degrees of freedom. The energy dependence of the ratio of the total number of produced s and $\bar{s}$ quarks (as deduced from strange particle yields) to pions is plotted in Fig. 2, *b*. It exhibits a sharp peak at low SPS energy with a fall-off to a lower plateau value consistent with the expectation for a deconfined phase (dash-dotted curve [1]). The described features are neither seen in $p + p$ collisions (open dots) nor in purely hadronic

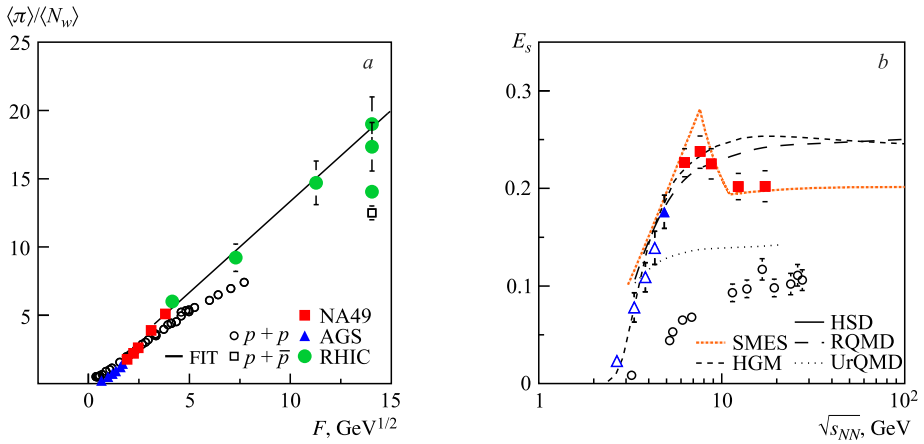

Fig. 2. *a*) Total pion yield $\langle\pi\rangle$ divided by the number of wounded nucleons $\langle N_W\rangle$ versus collision energy in central Pb + Pb and Au + Au compared to $p + p$ collisions (the Fermi variable $F \approx s_{NN}^{0.25}$ GeV$^{0.5}$ is used). *b*) Ratio $E_S = (\langle K\rangle + \langle\Lambda\rangle)/\langle\pi\rangle$ of total number of strangeness carriers to pions versus collision energy

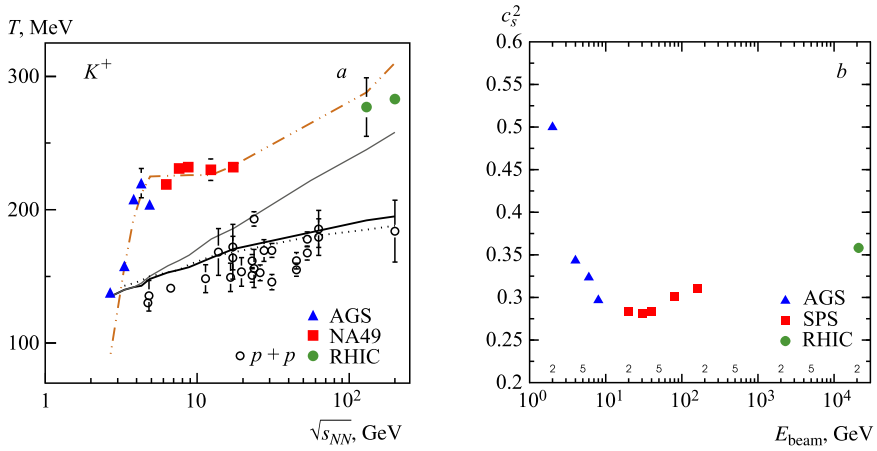

Fig. 3. *a*) Inverse slope parameter T of the invariant transverse mass distribution of K^+ mesons versus collison energy. Square symbols show NA49 results and are compared to measurements at lower and higher energies. Open circles show measurements in $p+p$ reactions. The curves show various model predictions (see text). *b*) Sound velocity c_s in the fireball as determined from the width of the pion rapidity distribution using the Landau hydrodynamic model [16] versus energy

model calculations using microscopic transport models (UrQMD [11] and HSD [12]) or the statistical hadron gas model (HGM [13]). Extensions of the HGM [10] provide a better description of the data with a hypothetical exponential high mass hadron spectrum which can be considered equivalent to deconfinement.

A phase transition is expected to also manifest itself in the momentum distributions and correlations of produced particles [14]. A plot of the inverse slope parameter T of the invariant transverse mass distribution of K^+ mesons at midrapidity is shown in Fig. 3, *a*. One observes a steep rise at low energies turning into a plateau at SPS energies which is not found in $p+p$ reactions. This feature, also found for pions, protons and antiprotons [2], cannot be described by available hadronic models and suggests the onset of the phase transition with hadronisation through an intermediate mixed phase. A microscopic model incorporating a first-order transition [15] can in fact reproduce the measurements (dash-dotted curve). The softness of the equation of state near the onset of deconfinement is also seen as a minimum in the sound velocity c_s (see Fig. 3, *b*) derived from the width of pion rapidity distributions using the Landau hydrodynamic model [16].

In summary, the observed energy dependence of hadron production properties in central collisions of heavy nuclei shows anomalies at low SPS energies which are most naturally explained by the onset of deconfinement in the early stage of the produced fireball for beam energies of about $30A$ GeV.

2. SEARCH FOR THE CRITICAL POINT OF STRONGLY INTERACTING MATTER AT THE SPS

The presence of the predicted critical point is expected to lead to an increase of event-by-event fluctuations of many observables [5–7] provided that the freeze-out of the measured hadrons occurs close to its location in the phase diagram and that the evolution of the

final hadron phase does not erase the fluctuation signals. As seen in Fig. 1, *a*, freeze-out at SPS energies does occur close to the predicted phase boundary and the critical point. The size of critical fluctuations depends on the correlation length ξ, which diverges in the ideal case [5]. However, due to the finite size (radius about 7 fm) and lifetime (few fm/c) of the system created in collisions of heavy nuclei, correlation lengths are expected to remain below about 6 fm [6, 7]. The NA49 and NA61 experiments follow the strategy of changing the energy and size of nuclei in order to scan the phase diagram and look for a maximum in fluctuations as experimental signature for the critical point (see Figs. 1, *b* and 9, *b*). In the following, measurements from NA49 at the SPS will be discussed and compared to theoretical expectations and to results from RHIC.

Particle multiplicity fluctuations are characterized by the scaled variance ω of the multiplicity distribution, while $\langle p_T \rangle$ fluctuations can be quantified by the Φ_{p_T} measure. System size and energy dependence of ω [17, 18] and Φ_{p_T} [18, 19] are shown in Fig. 4. Results for different energies and nuclear masses are plotted as function of baryochemical potential μ_B and temperature $T_{\rm chem}$ extracted from the hadron gas model fits to particle yields (see above).

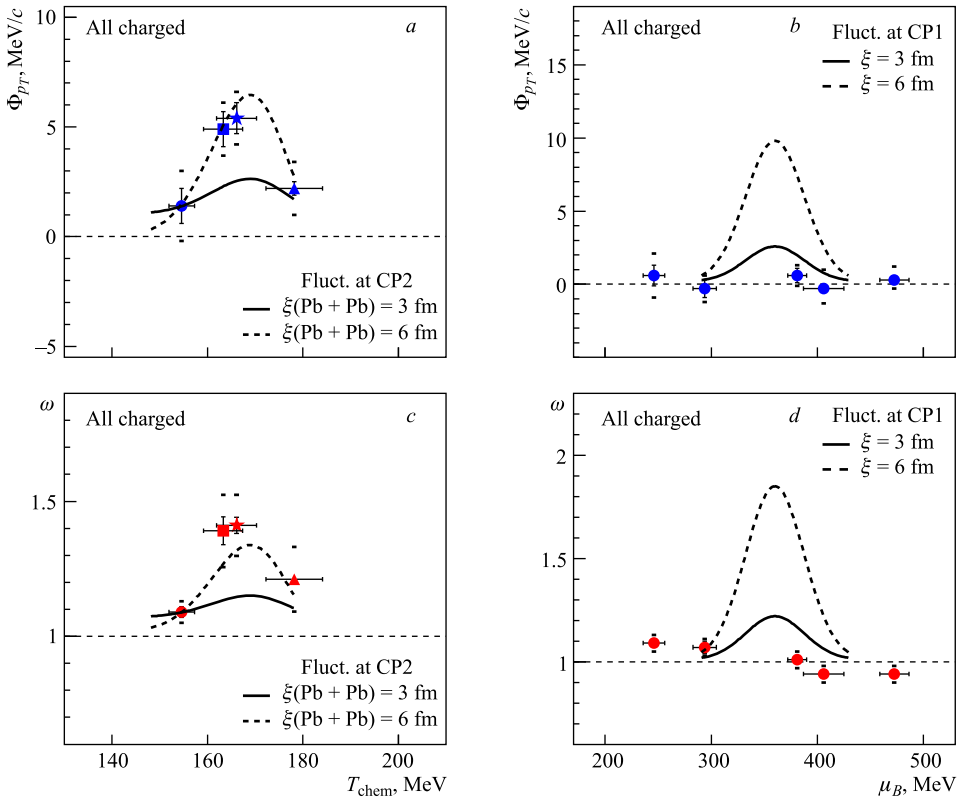

Fig. 4. Fluctuation measures Φ_{p_T} of average transverse momentum and the scaled variance ω of the multiplicity distribution versus freeze-out temperature T and baryochemical potential μ_B measured by NA49. Dashed and solid lines indicate the estimated effects of the critical point for two values of the correlation length ξ

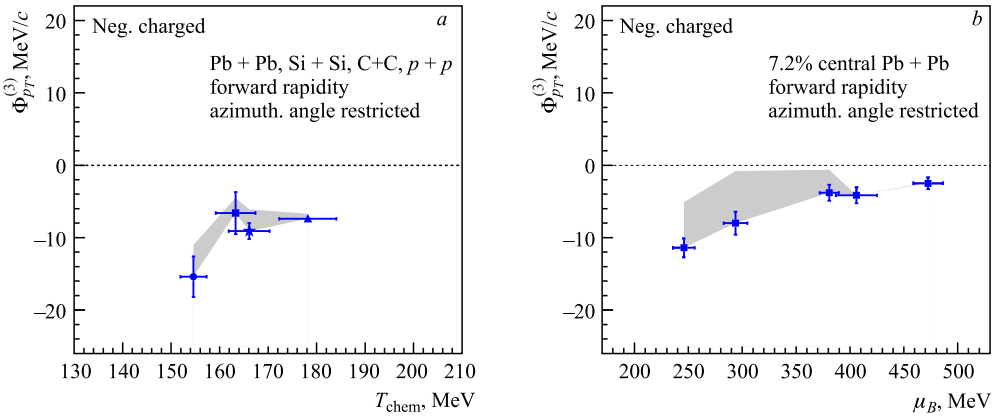

Fig. 5. Third moment $\Phi^{(3)}_{p_T}$ of average transverse momentum fluctuations versus T (*a*) and μ_B (*b*) for negatively charged particles (NA49 preliminary)

Experimental results for the μ_B and $T_{\rm chem}$ dependence are compared to the estimated effect of the critical point [6] for two hypothetical locations: CP1 ($T = 147$ MeV, $\mu_B = 360$ MeV) and CP2 ($T = 178$ MeV, $\mu_B = 250$ MeV), respectively. No indications of a maximum is observed in the energy dependence. However, a peak consistent with theoretical predictions may develop in the $T_{\rm chem}$ dependence at the highest SPS energy for collisions of lighter nuclei. Higher moments of fluctuations are expected to show larger effects [6], but are unfortunately also more sensitive to experimental background. Figure 5 shows measurements of the third moment $\Phi^{(3)}_{p_T}$ [20] of $\langle p_T \rangle$ fluctuations for negatively charged hadrons (providing the cleanest track sample). No evident maximum is observed.

Event-by-event fluctuations of azimuthal angle are believed to be sensitive to plasma instabilities [21], fluctuations of elliptic flow [22] as well as the presence of the critical point. NA49 results on energy and system size dependence of azimuthal angle fluctuations are plotted in Fig. 6. A featureless energy dependence is observed, whereas a weak indication of a maximum is visible in the nuclear size dependence.

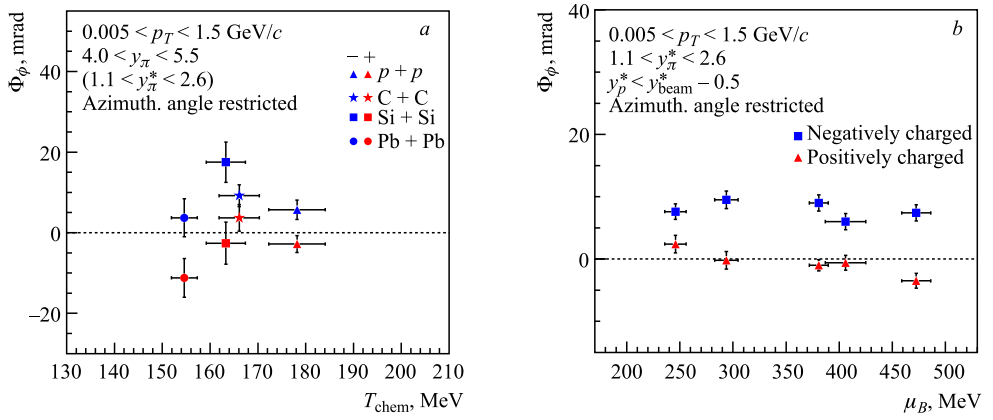

Fig. 6. Φ_ϕ measure of fluctuations of the average azimuthal angle versus T (*a*) and μ_B (*b*) for negatively (blue upper points) and positively (red lower points) charged particles (NA49 preliminary)

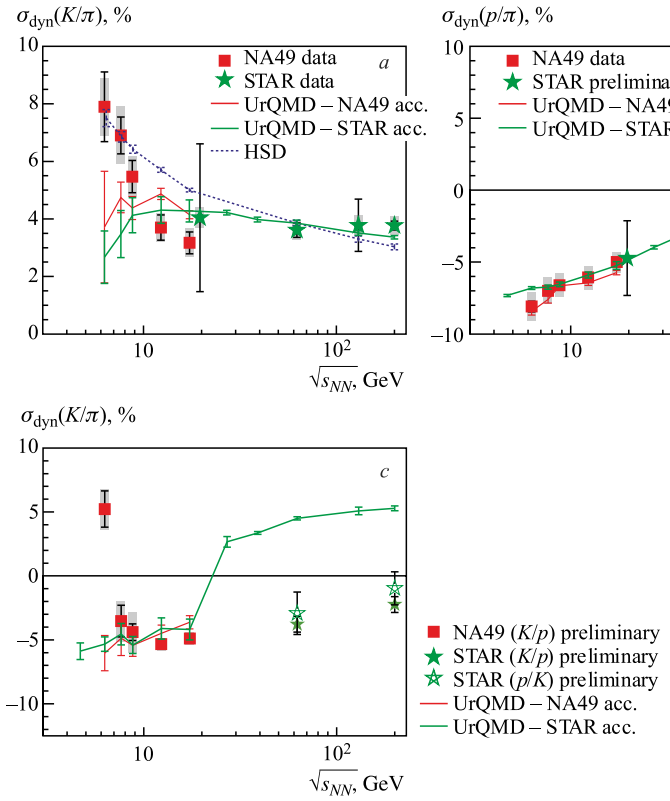

Fig. 7. Fluctuations of particle ratios measured by $\sigma_{\rm dyn}$ for K/π (*a*), p/π (*b*) and K/p (*c*) in central collisions of Pb + Pb (NA49 — squares) and Au + Au (STAR — stars) collisions. Curves show model predictions

Event-by-event fluctuations of particle ratios may also be sensitive to phase transitions and the critical point. Results from NA49 for the measure $\sigma_{\rm dyn} = {\rm sign}\,(\sigma^2_{\rm data} - \sigma^2_{\rm mix})\sqrt{|\sigma^2_{\rm data} - \sigma^2_{\rm mix}|}$ are shown in Fig. 7 and compared to measurements from the STAR experiment. Here $\sigma^2_{\rm data}$ and $\sigma^2_{\rm mix}$ are the widths of distributions of particle ratios for real and mixed events, where the latter estimate the statistical background. K/π fluctuations (Fig. 7, *a*) exhibit a strong rise towards the lowest SPS energy. This has been interpreted as a consequence of the decreasing particle multiplicities [25]. However, the hadronic model calculations do not provide unambiguous confirmation. On the other hand, the rise may be related to the onset of deconfinement since the ratio of yields of kaons to pions changes. For the p/π ratio (Fig. 7, *b*) one observes negative values of $\sigma_{\rm dyn}$ which can be explained by the effect of nucleon resonances as suggested by the UrQMD model calculations. The values of $\sigma_{\rm dyn}$ for the K/p ratio (Fig. 7, *c*) change sign as the energy decreases. This result may be related to the correlation coefficient $C_{\rm BS}$ which is smaller in the hadron phase than in the QGP [26].

At the critical point local density fluctuations with power-law singularity are expected in both configuration and momentum space [27] and should appear both for baryonic density

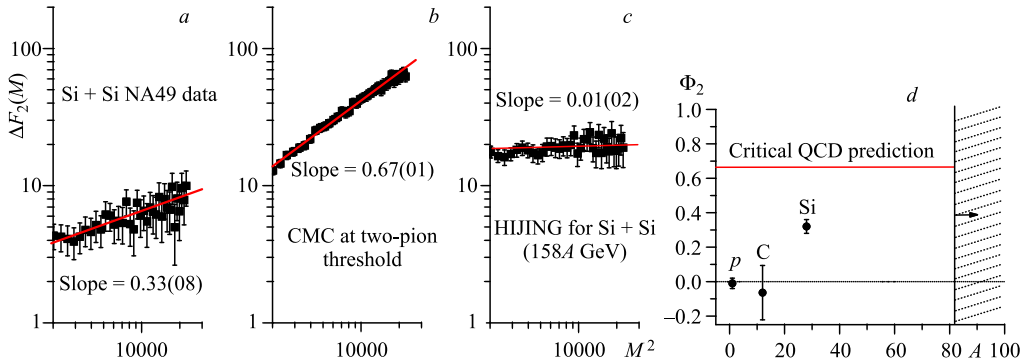

Fig. 8. *a–c*) Factorial moments ΔF_2 for low-mass $\pi^+\pi^-$ pairs in central Si + Si collisions at 158A GeV for data (*a*), simulation of critical fluctuations (*b*) and the HIJING model (*c*). *d*) Intermittency index Φ_2 for various collisions studied by NA49

and for the σ field. Critical σ fluctuations are predicted to be observable as intermittency behaviour of the factorial moments of the density of low-mass $\pi^+\pi^-$ pairs in transverse momentum space: $\Delta F_2(M) \propto M^{2\Phi_2}$. Results for central Si + Si collisions at top SPS energy are plotted in Fig. 8, *a–c*. There is a clear intermittency signal in the data (plot *a*), somewhat weaker than in a simulation of critical behaviour (plot *b*), while there is no signal in a typical hadronic model (plot *c*). As shown in Fig. 8, *d* the effect disappears for smaller systems.

In summary, there is no convincing evidence for the critical point as yet, but several interesting indications strongly motivate the continuation of the search.

3. CONTINUATION OF THE SEARCH FOR THE CRITICAL POINT BY EXPERIMENT NA61 AT THE SPS

The NA61/SHINE experiment [8] will continue the program of NA49 with the main aim of searching for the critical point and studying in detail the onset of deconfinement by performing a two-dimensional scan of the phase diagram in T, μ_B (see Fig. 9, *b*). This will be achieved by varying collision energy (13A–158A GeV) and size of the colliding systems ($p+p$, $p+$Pb, B + C, Ar + Ca, Xe + La). In addition to these main objectives, the experiment will measure the energy dependence of the nuclear modification factor of high-p_T particle production at the SPS and obtain precision data on hadron spectra in hadron–nucleus collisions for the T2K neutrino experiment, and for the Pierre Auger Observatory and KASCADE cosmic-ray experiments.

Several upgrades of the detector apparatus inherited from NA49 are completed or in progress (see Fig. 9, *a*). In 2007, a forward Time-of-Flight system was constructed in order to extend the acceptance for particles with momenta < 3 GeV/c. In 2008, the DAQ system and the TPC readout electronics were replaced, resulting in an increase of the data taking rate by a factor of 10. In 2011, a new Projectile Spectator Detector will be completed to replace the NA49 Forward Calorimeter. It will provide single-nucleon energy resolution which will be essential for the fluctuation studies. For 2011, the H2 beam line will be converted into a fragment separator to allow one to run with low-mass ions (boron) in parallel with the LHC Pb program.

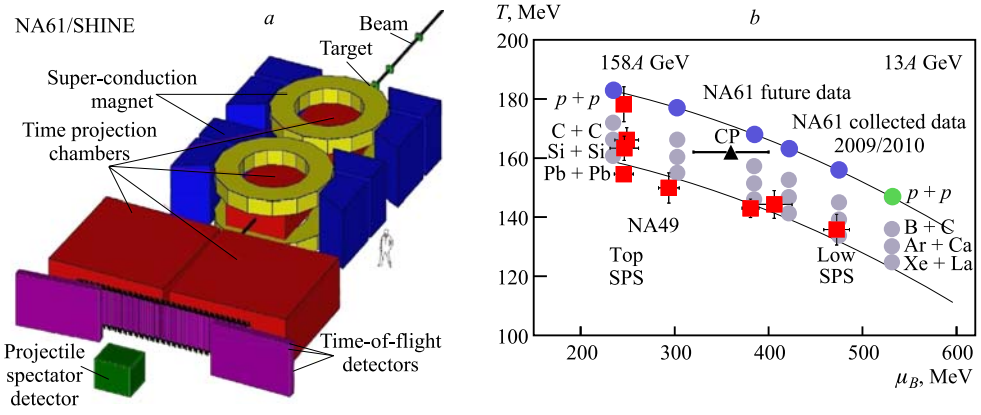

Fig. 9. *a*) Layout of experiment NA61/SHINE at the CERN SPS. *b*) Scan of the phase diagram by varying collision energy (μ_B) and size of colliding nuclei (T). Squares show the freeze-out points covered by NA49, circles indicate the planned measurements of NA61. The estimated location of the critical point is shown by the triangle

The first part of the system size and energy scan program, namely $p+p$ collisions at 13, 20, 30, 40, 80 and 158 GeV/c beam energy were/will be recorded in 2009, 2010 and 2011. B + C, Ar + Ca and Xe + La runs are foreseen for 2011, 2013 and 2014, respectively.

CONCLUSION

The energy dependence of hadron production properties are most naturally explained by the onset of deconfinement in the SPS energy range. So far only a tantalising indication but no convincing evidence has been found for the critical point of strongly interacting matter. A vigorous experimental program is continuing the search: NA61/SHINE at the SPS, the STAR experiment at RHIC, and future planned facilities MPS at NICA (2016) and CBM at FAIR (2017/2019).

REFERENCES

1. *Gazdzicki M., Gorenstein M.* // Acta Phys. Polon. B. 1999. V. 30. P. 2705.
2. *Alt C. et al. (NA49 Collab.)* // Phys. Rev. C. 2008. V. 77. P. 024903.
3. *Gazdzicki M., Gorenstein M., Seyboth P.* Preprint. arXiv:1006.1765. 2010.
4. *Fodor Z., Katz S.* // J. High Energy Phys. 2004. V. 0404. P. 50.
5. *Stephanov M., Rajagopal K., Shuryak E.* // Phys. Rev. D. 1999. V. 60 P. 114028.
6. *Stephanov M.* // Phys. Rev. Lett. 2009. V. 102. P. 032201;
   Stephanov M. Private communication. 2009.
7. *Berdnikov B., Rajagopal K.* // Phys. Rev. D. 2000. V. 61. P. 105017.
8. *Antoniou et al. (NA61 Collab.).* Proposal CERN-SPSC-2006-034/P-330 and addenda.
9. *Becattini F. et al.* // Phys. Rev. C. 2004. V. 69. P. 024905;
   Becattini F. et al. // Phys. Rev. C. 2006. V. 73. P. 044905.

10. *Andronic A., Braun-Munzinger P., Stachel J.* // Phys. Lett. B. 2009. V. 673. P. 142.
11. *Bass S. et al.* // Prog. Part. Nucl. Phys. 1998. V. 41. P. 225.
12. *Cassing W. et al.* // Nucl. Phys. A. 2000. V. 674. P. 249.
13. *Cleymans J., Redlich K.* // Phys. Rev. C. 1999. V. 60. P. 054908;
Braun-Munzinger P. et al. // Nucl. Phys. A. 2002. V. 697. P. 902.
14. *van Hove L.* // Phys. Lett. B. 1982. V. 89. P. 253;
Gorenstein M. et al. // Phys. Lett. B. 2003. V. 567. P. 175.
15. *Hama S. et al.* // Braz. J. Phys. 2004. V. 34. P. 322.
16. *Petersen H., Bleicher M.* // Proc. of Sci. 2006. CPOD2006. P. 25.
17. *Alt C. et al. (NA49 Collab.)* // Phys. Rev. C. 2008. V. 78. P. 034914.
18. *Grebieszkow K. (NA49 Collab.).* Preprint. arXiv:0907.4101. 2009.
19. *Anticic T. et al. (NA49 Collab.)* // Phys. Rev. C. 2009. V. 79. P. 044904.
20. *Mrowczynski S.* // Phys. Lett. B. 1999. V. 465. P. 8.
21. *Mrowczynski S.* // Phys. Lett. B. 1993. V. 314. P. 118.
22. *Mrowczynski S., Shuryak E.* // Acta Phys. Polon. B. 2003. V. 314. P. 4241.
23. *Cetner T., Grebieszkow K. (NA49 Collab.).* Preprint. arXiv:1008.3412. 2010.
24. *Alt C. et al. (NA49 Collab.)* // Phys. Rev. C. 2009. V. 79. P. 044910;
Anticic C. et al. (NA49 Collab.).[1] Preprint. arXiv:1101.3250. 2011.
25. *Koch V., Schuster T.* // Phys. Rev. C. 2010. V. 81. P. 034910.
26. *Koch V.* // Phys. Rev. Lett. 2005. V. 95. P. 182301.
27. *Antoniou N. et al. (NA49 Collab.)* // Nucl. Phys. A. 2005. V. 761. P. 149.
28. *Anticic T. et al. (NA49 Collab.)* // Phys. Rev. C. 2010. V. 81. P. 064907.

[1] UrQMD calculations at $\sqrt{s_{NN}} > 20$ GeV were provided by Hui Wang, MSU.